

RESEARCH

Open Access



# Weighted average current method for active damping control based on grid voltage feed-forward

Shengqing Li<sup>1,2\*</sup>, Xinluo Li<sup>1</sup> and Xiaobao Lee<sup>1</sup>

## Abstract

In the weak current network environment, the existence of power network impedance will reduce the current control stability margin of LCL grid connected inverter, the stability margin will gradually deteriorate as the inductive component of the power network impedance increases, leading to system instability. In this paper, an improved weighted average current control strategy is proposed, which is based on the active damping control of the voltage feedforward of the charged network. In the new control strategy, with the zero-pole cancellation method, a new weighting coefficient related only to the parameters of LCL filter is obtained, which reduces the order of the system, suppresses the influence of power network impedance, and improves the stabilization of the system, getting better inverter output current quality. Then the influence of power network impedance on the control system of grid connected inverter is analyzed, and the feed-forward control of grid voltage is improved to improve the stability of inverter in weak current network. The Bode diagram analysis and MATLAB simulation results proved that the proposed control strategy is feasible.

**Keywords:** Weak grid, Weighted average current, Zero pole cancellation, System reduction, Grid impedance, Resonant frequency

## Introduction

Large-scale power generation equipment connected to long-range load centers through long-distance transmission lines has many technical challenges [1]. In the process of actual long-distance transmission, a large number of line impedances will be introduced in the power grid. Under the joint action of these line impedances and non-linear loads, the grid impedances can be overlooked, where the power grid is called weak grid [2–4], and the power grid generally has many inductive components within a certain frequency range [5, 6]. The grid-connect inverter will reduce the stability of the system when considering the power network impedance. Therefore, the research on the control strategy of a grid

connected inverter in the weak grid has gradually become the focus of scholars all over the world.

Weighted average current control, as a damping control strategy, has received extensive attention due to its ring-like order reduction characteristics [7–9]. Grid pattern considering the influence of impedance is equal to the form of resistance series inductance, and the influence of impedance on grid-connect system is analyzed [10]. In reference [11], Zhou Lin et al. converted the mathematical model of the three-phase LCL inverter into the Norton equivalent circuit form, discusses the relationship between the grid-connected current and the voltage at the common coupling point, and obtains the closed-loop transfer function of the grid-connected system, and then uses Routh's decision table and root locus method analyze the stability of its system, which lays a theoretical foundation for the inverter control scheme under weak grid. Xu Jinming and his colleagues [12]

\* Correspondence: [lsq1961@sohu.com](mailto:lsq1961@sohu.com)

<sup>1</sup>School of Electrical and Information Engineering, Hunan University of Technology, Zhuzhou City 412007, Hunan Province, China

<sup>2</sup>Photovoltaic micro-grid intelligent control technology Hunan Engineering Research Center, Zhuzhou 412007, Hunan, China

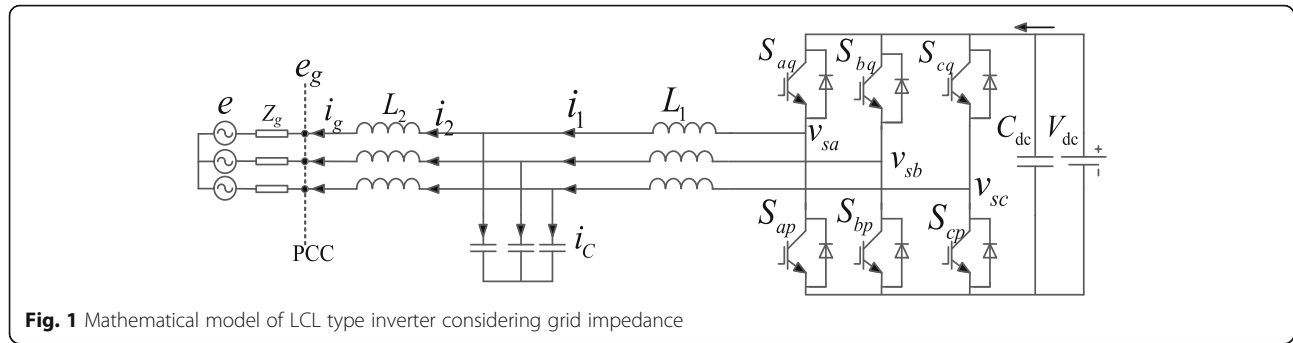


**Fig. 1** Mathematical model of LCL type inverter considering grid impedance

through in-depth analysis of the influence of the grid voltage feedforward control on the double closed-loop control of the filter capacitor current and the grid-connected current in a weak grid, an adaptive current control method for grid impedance estimation is proposed, which can dynamically update the regulator parameters. Adapt to the characteristics of weak power grids, but the dynamic measurement of power grid impedance makes the control system design more complicated and difficult to implement. In Reference [13], Yang Dongsheng et al. used virtual series impedance and virtual parallel impedance to adjust the phase angle and modulus of the inverter output impedance. The requirements of robustness and anti-interference performance can be considered at the same time, and the adaptability of the inverter to the weak power grid is improved. In Reference [14, 15] First, the AC is fed forward by adding resonance to the grid voltage, and then the fundamental voltage is extracted for feedforward control. Finally, it is combined with the quasi-PR controller and the resonance controller to better reduce the grid current harmonics. Xu Jinming and his colleagues [16] analyzed The influence of the grid impedance on the control system of the grid-connected inverter is analyzed, and the grid voltage feedforward control is improved to improve the stability of the inverter in a weak grid. Active damping of LCL filter is very important to control LCL grid-connect inverter. Active damping can reduce the resonance peak caused by LCL filter and stabilize the whole system easily [17–19]. In their work, a current weighted feed-back on-line inductive reactance detection technology is adopted. After dynamic measurement of inductive reactance, the weighting coefficient is adjusted to improve the performance of current weighted control and improve the robustness of the system [20].

In this article, based on the active damping control of grid voltage feed-forward, the weighted average current method is introduced to design a new weighting coefficient, which can restrain the influence of the inductive

component in the grid impedance, reduce the system order and improve the stabilization of the system.

### LCL grid connected inverter mathematical pattern

Figure 1 is the mathematical pattern of LCL three-phase grid-connect inverter considering the existence of grid impedance, where  $e$  is three-phase grid voltage,  $v_{sk}$  ( $k = a, b, c$ ) is inverter-side voltage,  $S_{aq}$ 、 $S_{ap}$ 、 $S_{bq}$ 、 $S_{bp}$ 、 $S_{cq}$ 、 $S_{cp}$  are six IGBT,  $V_{dc}$  is DC voltage,  $C_{dc}$  is DC capacitance,  $L_1$  is inverter side inductance,  $L_2$  is grid-side inductance,  $i_1$  is inverter side current,  $i_2$  is grid side current,  $i_c$  is filter capacitor current,  $Z_g$  is the grid impedance,  $e_g$  is the Common Coupling Point (PCC) voltage, and  $e_g$  includes the grid voltage and the voltage on the grid impedance  $Z_g$ .

According to Fig. 1, the grid impedance and common coupling point voltage are expressed as follows.

$$Z_g = r_g + sL_g \quad (1)$$

$$e_g = e + Z_g * i_2 \quad (2)$$

In eqs. (1) and (2),  $r_g$  and  $L_g$  are the resistive and inductive components of the grid impedance, respectively, and  $L_g = \beta(L_1 + L_2)$ ,  $\beta$  is the percentage of the inductive component of the power network impedance in the total inductance of the inverter.

**Table 1** Inverter default parameters

Related parameter	Value
Grid voltage effective value $eg/V$	220
Grid voltage frequency $f/Hz$	50
DC side bus voltage $V_{dc}/V$	680
switching frequency $f_s/kHz$	20
Rated power $P/kw$	12
Inductance at inverter side $L_1/\mu H$	500
Grid side inductance $L_2/\mu H$	600
Filter capacitance $C/\mu F$	8

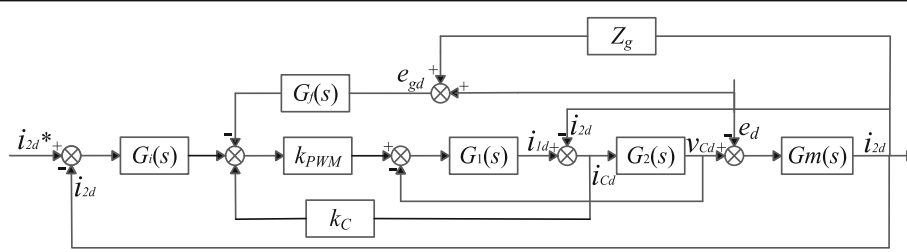


**Fig. 2** Active damping control block diagram based on grid voltage feed-forward

This paper will take a three-phase grid-connect inverter as an example for analysis, and its related parameters are shown in Table 1.

**Analysis of active damping control scheme based on grid voltage feedforward**

Figure 2 is the double closed-loop current control block diagram based on grid voltage feed-forward, in which  $k_C$  is the feedback coefficient and  $k_{PWM}$  is the PWM inverter link. In this paper, we use SVPWM modulation,

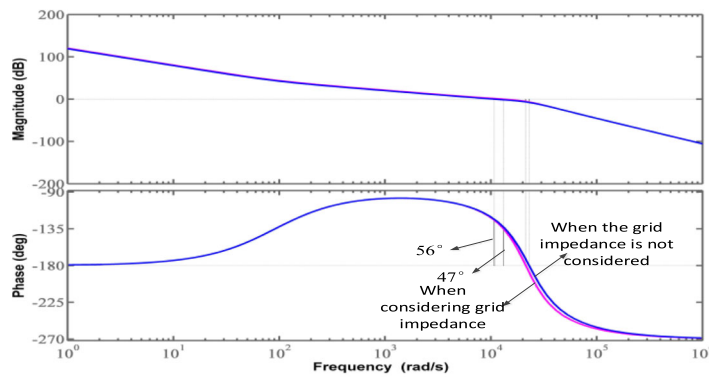
in which the value of  $k_{PWM}$  is 1 and  $G_f(s)$  is the feed-forward coefficient.

From Fig. 2, the open-circuit transfer function of grid-connect current can be expressed as follows

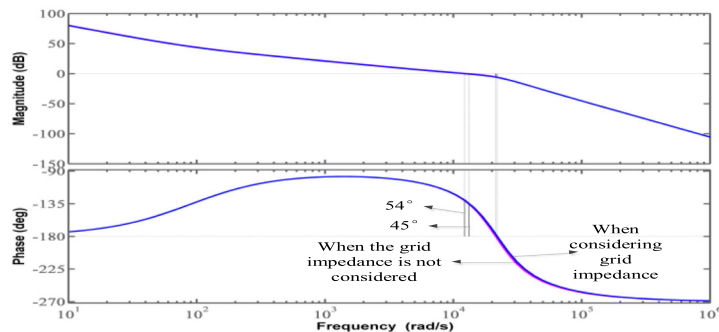
$$G_{i2.O} = \frac{k_{PWM}G_i(s)G_1(s)G_m(s)G_2(s)}{1 + G_1(s)G_2(s)k_{PWM}k_CG_2(s)G_m(s) - G_f(s)Z_gk_{PWM}G_1(s)G_2(s)G_m(s)} \tag{3}$$

where,  $G_i(s)$  is PI controller,  $G_1(s) = 1/sL_1$ ,  $G_2(s) = 1/sC$ ,  $G_m(s) = 1/(sL_2 + Z_g)$ ,  $G_f(s) = 1/k_{PWM}$ ,  $k_C = 10.7$ .

It can obtain the relationship by expanding the eq. (3):

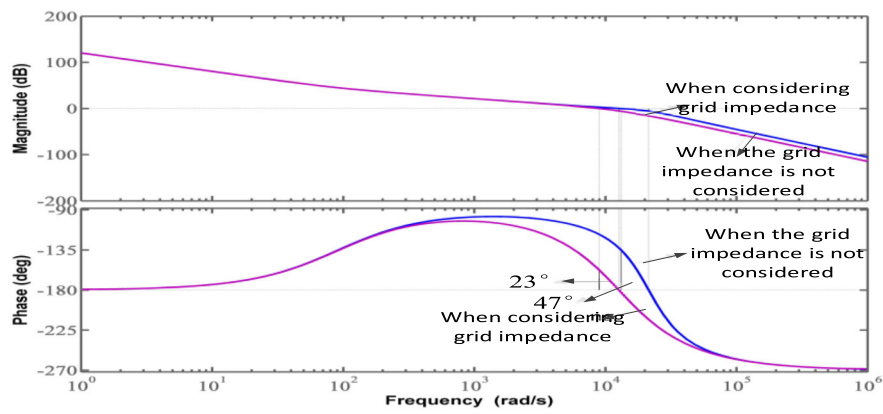


(a)  $r_g = 0.7\Omega$

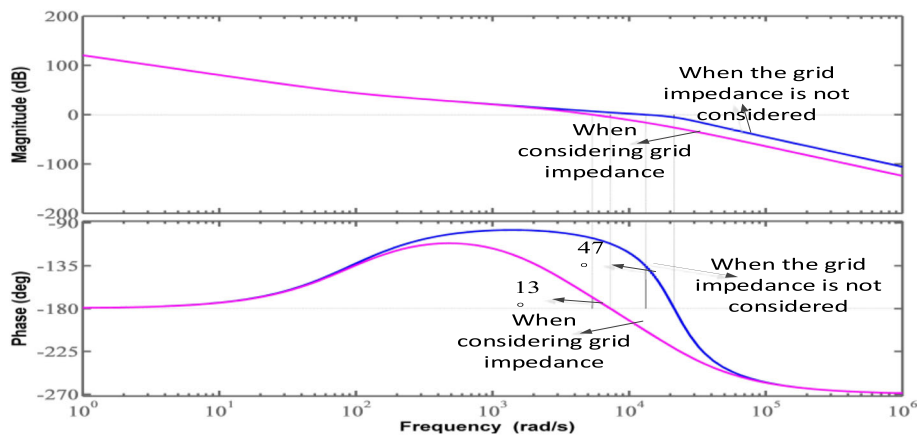


(b)  $r_g = 2\Omega$

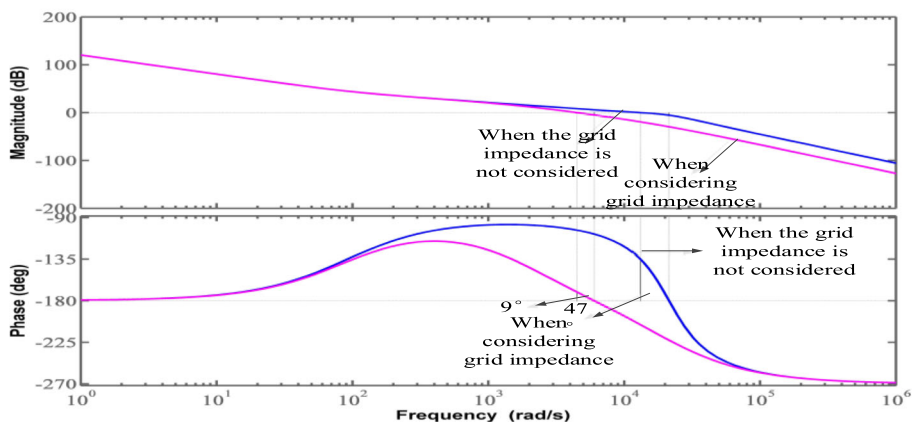
**Fig. 3** Bode diagram of active damping control based on grid voltage feedforward under pure resistance. **a**  $r_g = 0.7\Omega$ . **b**  $r_g = 2\Omega$



( a )  $\beta=1$



( b )  $\beta=4$



( c )  $\beta=6$

**Fig. 4** Bode diagram of active damping control based on grid voltage feed-forward under pure inductance. **a**  $\beta=1$ . **b**  $\beta=4$ . **c**  $\beta=6$

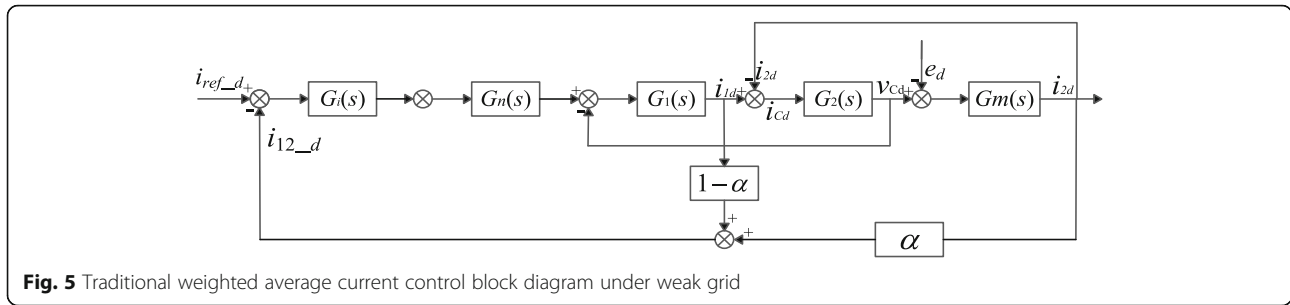


Fig. 5 Traditional weighted average current control block diagram under weak grid

$$G_{i2.O} = \frac{G_i(s)kPWM}{s^2L_1C(sL_2 + Z_g) + kPWMkcsC(sL_2 + Z_g) + s(L_1 + L_2) + Z_g - Z_gG_f(s)kPWM} \tag{4}$$

$$\omega_{z_g} = \sqrt{\frac{L_1 + L_2}{L_1(L_2 + L_g)C}} \tag{6}$$

If  $G_f(s) = 1/s$  is introduced into eq. (4), then:

$$G_{i2.O} = \frac{G_i(s)kPWM}{s^2L_1C(sL_2 + Z_g) + kPWMkcsC(sL_2 + Z_g) + s(L_1 + L_2)} \tag{5}$$

When the power network impedance is pure resistance, Bode diagram of double current closed-loop control based on grid voltage feedforward can be obtained through the eq. (5), as shown in Fig. 3, with  $r_g = 0.7$  and  $2 \Omega$ , corresponding to Fig. 3a and b, respectively.

Obviously, if the grid impedance is pure resistance, the Bode diagram of the system changes very little, and the marginal changes only a few degrees, if the resistance increases, the phase margin of the system decreases slightly, with little change range, and the phase frequency curve basically coincides. Therefore, when the impedance is pure resistance, it has little effect on the system and it still runs stably, this is the influence of the resistive component in the power network impedance on the system, which can be almost ignored.

When the grid impedance is pure inductance, the frequency of conjugate open-circus poles of the system can be obtained from eq. (5) as follows

From eq. (6), we can get the Bode diagram of active damping control based on grid voltage feed-forward under pure inductance, as shown in Fig. 4.

It can be seen from Fig. 4 and eq. (6) that the resonance frequency of the system will decrease with the increase of the inductive reactance of the power grid, and the decrease of the resonance frequency has a very obvious attenuation effect on the phase margin. Therefore, as the power grid's inductive reactance increases, the margin of the system will always decrease until the grid connected system of the inverter loses its stability completely, so the existence of the inductive impedance of the power grid has a large impact on the feed-forward active damping control because of the large noise, it is necessary to suppress the influence of grid impedance.

### Control strategy

Through the above analysis, we know that when the grid impedance exists, and because of the truth that the inductive component will have a great impact on the feed-forward control, while the resistive component can be ignored. Therefore, in order to ensure the stable operation of the system in the weak current network environment, here we introduce the weighted average current method to suppress the effect of the power network

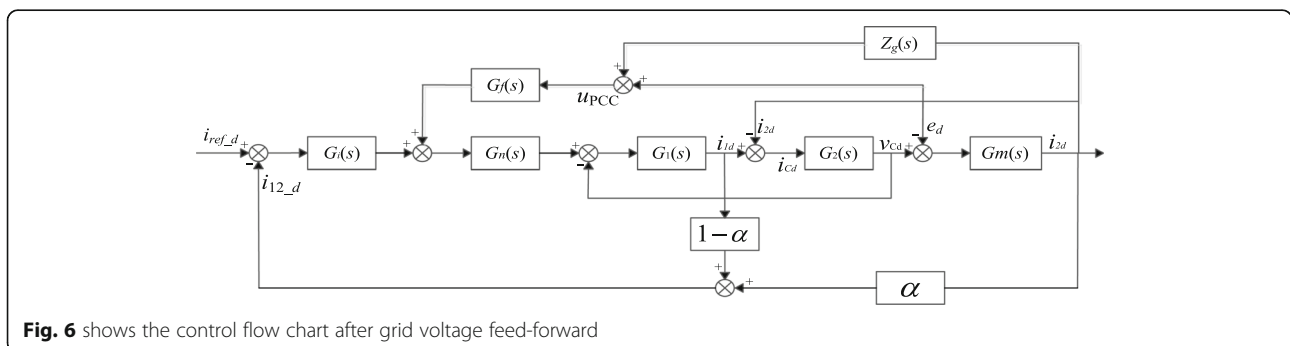


Fig. 6 shows the control flow chart after grid voltage feed-forward

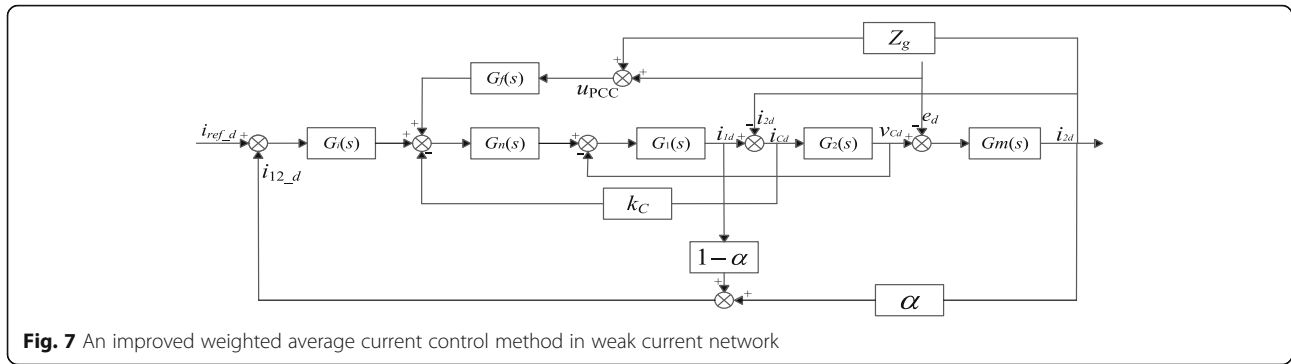


Fig. 7 An improved weighted average current control method in weak current network

impedance based on the active damping control of power network voltage feed-forward.

**Traditional weighted average current control strategy**

The principle of the weighted average current strategy is to sum the part of grid-connect current and the inverter side current by weight, then take it as the feed-back value of the input current, which can not only ensure the tracking accuracy of the system, but also make the system have a higher power factor. The weighted average current traditional control flow chart under the weak current network is shown in Fig. 5, and the  $i_{12}$  in the figure meets the relationship.

$$i_{12\_d} = (1 - \alpha) i_1 + \alpha i_{2d} \tag{7}$$

Where  $i_1$  is inverter side current,  $i_2$  is grid connection current,  $i_{12\_d}$  is weighted average current and  $\alpha$  stand for weighting factor.

From Fig. 5, we can get the open-circus transfer function  $G_{open}$  from  $i_{ref\_d}$  to  $i_{12\_d}$

$$G_{open} = \frac{i_{12\_d}}{i_{ref\_d}} = \frac{G_i(s)k_{PWM}[(1 - \alpha)s^2C(L_2 + L_g) + 1]}{s^3L_1C(L_2 + L_g) + s(L_2 + L_1 + L_g)} \cdot \frac{G_i(s)k_{PWM}[(1 - \alpha)s^2C(L_2 + L_g) + 1]}{G_i(s)k_{PWM}[(1 - \alpha)s^2C(L_2 + L_g) + 1]} = \frac{1}{(L_g + L_1 + L_2) \left[ 1 + \frac{L_1}{L_g + L_1 + L_2} (L_2 + L_g)Cs^2 \right]} \tag{8}$$

Considering the inductive reactance of the power grid, the weighting coefficient of traditional weighted average current is designed as follows

$$\alpha = 1 - \frac{L_1}{L_g + L_1 + L_2} = \frac{L_g + L_2}{L_g + L_1 + L_2} \tag{9}$$

The control blocks diagram after introducing the grid voltage feedforward is shown in Fig. 6. It can be seen that after considering the grid voltage feed-forward, the grid side voltage forms an additional positive feedback path through the grid inductive reactance  $L_g$ . This path does not exist in the strong power grid, and the additional positive feedback path will have an impact on the weighting coefficient.

In Fig. 6, the open-circus transfer function from  $i_{ref\_d}$  to  $i_{12\_d}$  is as follows

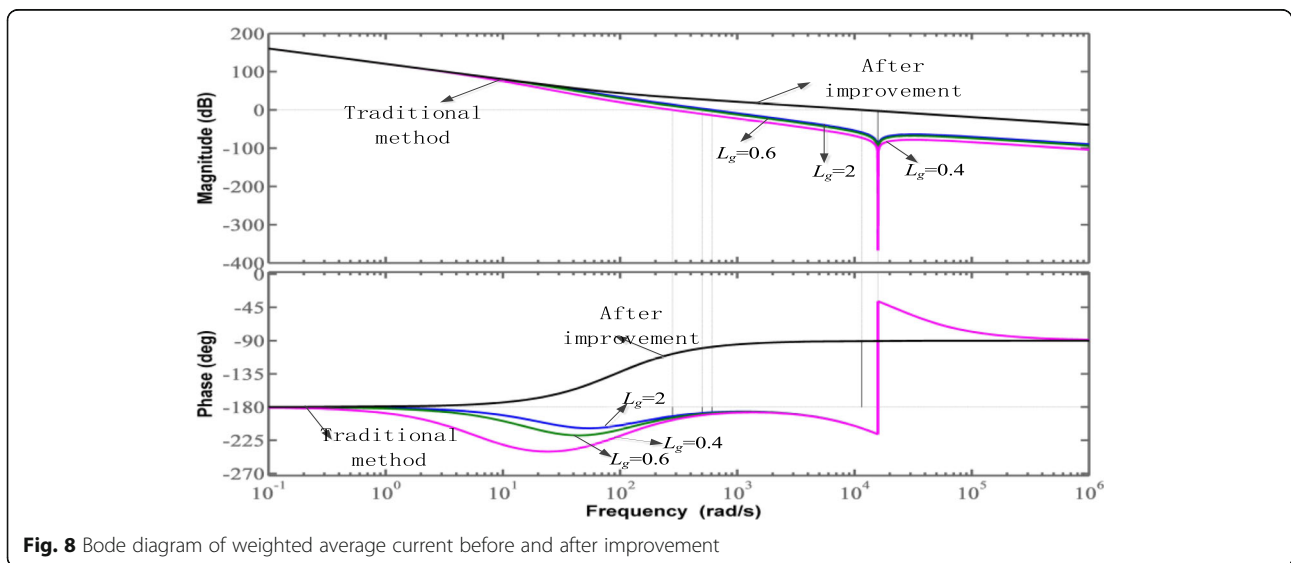


Fig. 8 Bode diagram of weighted average current before and after improvement

**Table 2** Closed-loop transfer function Rolls decision table

$s^2$	$(1-\alpha)(L_2 + L_g)C$	2
$s$	0	0
$s^0$	-	-

$$G_{open\_g}(s) = \frac{i_{12\_d}}{i_{ref\_d}} = \frac{G_i(s)k_{PWM}[(1-\alpha)(L_2 + L_g)Cs^2 + 1]}{L_1(L_2 + L_g)Cs^3 + (L_1 + L_2 + L_g)s - G_f(s)k_{PWM}L_g s} \tag{10}$$

Take the weighting coefficient of eq. (9) into eq. (10) to obtain

$$G_{open\_g} = \frac{i_{12\_d}}{i_{ref\_d}} = \frac{G_i(s)k_{PWM} \left[ \frac{L_1}{L_g + L_1 + L_2} s^2 C(L_2 + L_g) + 1 \right]}{s(L_g + L_1 + L_2) \left[ \frac{L_1}{L_g + L_1 + L_2} (L_2 + L_g) Cs^2 - \frac{G_f(s)k_{PWM}L_g}{L_g + L_1 + L_2} + 1 \right]} \tag{11}$$

It can be seen from eq. (11) that there is an additional term  $G_f k_{PWM} L_g / (L_1 + L_2 + L_g)$  in the transfer function of the system, and this term is related to the inductive reactance of the power grid. In order to reduce the system to the first order, this term must be eliminated. It is necessary to make  $G_f(s) = 0$ , that is to say, to eliminate the feed-forward term of the power grid voltage, and inductive reactance of the power grid will have an impact on the feed-forward term in the weak grid. Therefore, improved weighted average current control strategy is proposed.

**An improved weighted average current control strategy**

With the weighted average current method based on grid voltage feed-forward-based active damping control introduced, the control flow chart is shown in Fig. 7. As analyzed above, the grid voltage feed-forward link uses the grid impedance to introduce a positive feedback path to the control system block diagram, so the main idea of improving the adaptability of the weighted average current in a weak grid is to adopt a new weighting calculation method, then the system is reduced to the first-order form by the pole-zero cancellation method. Meanwhile, the regenerative feed-back circuit introduced by grid front feed is eliminated.

In Fig. 7, it can be concluded that the transfer function of the system  $i_{ref\_d}$  to  $i_{12\_d}$  is

$$G_{open\_g} = \frac{i_{12\_g}}{i_{ref\_g}} = \frac{G_i k_{PWM} [(1-\alpha)(L_g + L_2)Cs^2 + 1]}{L_1(L_g + L_2)Cs^2 + (L_1 + L_g + L_2)s + k_C k_{PWM} s^2 C(L_g + L_2) - G_f(s)k_{PWM}L_g s} \tag{12}$$

Substituting  $G_f(s) = 1/k_{PWM}$  into (12) can obtain

$$G_{open\_g}(s) = \frac{i_{12}}{i_{ref}} = \frac{G_i(s)k_{PWM} [(1-\alpha)(L_2 + L_g)Cs^2 + 1]}{s(L_1 + L_2)} = \frac{L_1}{L_1 + L_2} (L_2 + L_g)sC \left[ s + \frac{k_C k_{PWM}}{L_1} \right] + 1 \tag{13}$$

It can be seen from eq. (13) that in order to perform pole-zero cancellation, the circuit of  $k_C k_{PWM} (L_2 + L_g)s^2 C$  needs to be eliminated, so  $k_C = 0$ , namely, the capacitive current feedback circuit is not needed at this time. Then eq. (13) can be changed as

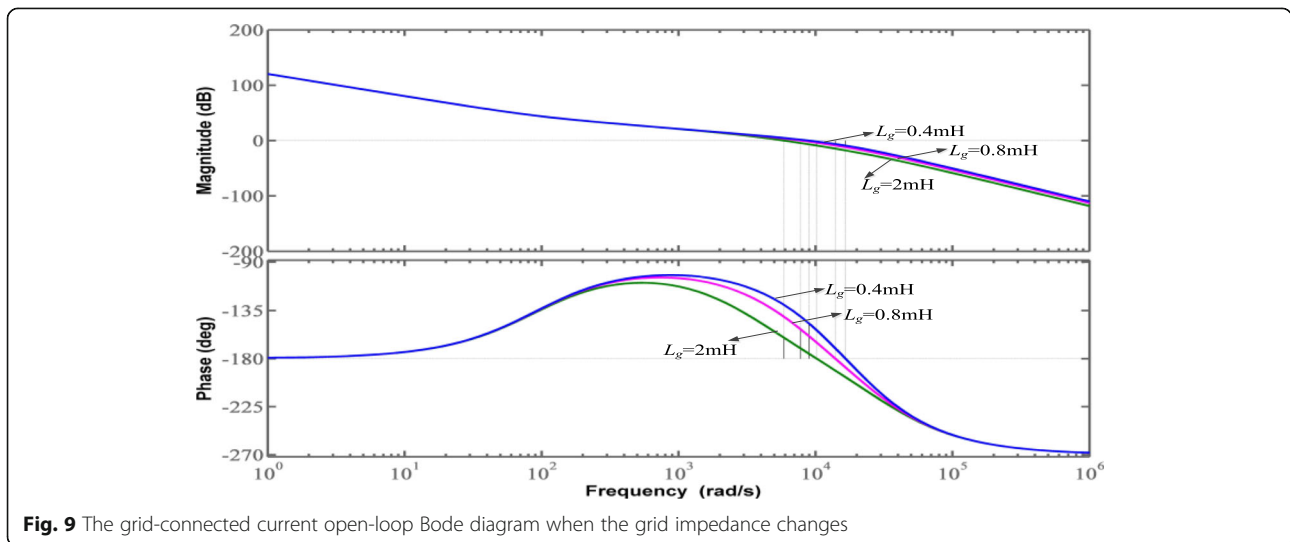


**Fig. 9** The grid-connected current open-loop Bode diagram when the grid impedance changes

$$G_{open\_g} = \frac{\frac{G_i(s)k_{PWM}}{s(L_1 + L_2)} [(1 - \alpha)(L_2 + L_g)Cs^2 + 1]}{\frac{L_1}{L_1 + L_2} (L_2 + L_g)s^2C + 1} \quad (14)$$

Obviously, the new weighting coefficient can be expressed as

$$\alpha = \frac{L_2}{L_1 + L_2} \quad (15)$$

After that the open-circus transfer function of the system is reduced to the first-order form, as follows

$$G_{open\_g} = \frac{G_i(s)K_{PWM}}{s(L_1 + L_2)} \quad (16)$$

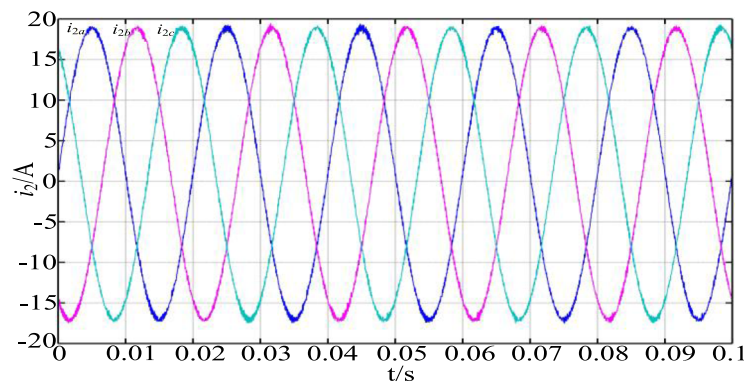
Equations (15)–(16) reveal that the current inner loop control is decreased from the third-order to the first-order, and is not affected by the grid impedance, and the weighting coefficient is completely determined by the parameters of the LCL filter.

From eqs. (11) and (16), it is easy to obtain Bode diagram of traditional weighted average current control and improved weighted average current control (see Fig. 8).

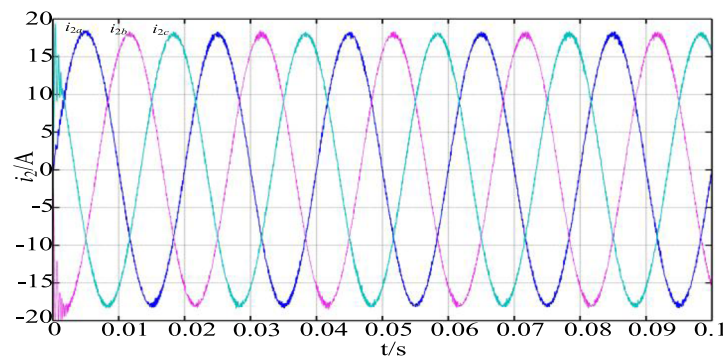
As shown in Fig. 8 when the grid impedance  $L_g = 0.4, 0.6$  and  $2$  mH. Under the traditional weighted average current, the system has resonance spikes, and the phase angle crosses  $-180$  degree, the system is unstable. However, the phase-frequency curve of the improved method changes with the impedance of the power grid, and the phase angle margin is always stable at about  $90$  degree, there is almost no change. The first-order characteristic is always maintained and being no longer affected by the power network impedance, the system can still operate stably.

### Stability analysis

In the improved weighted average current method, the transfer function from  $iref\_d$  to  $i12\_d$  is not affected by the grid impedance. However, the control target of the inverter is the grid current  $i_2$ , so it is necessary to analyze the grid current stability after improving the weighted average current.



(a) Grid-connect current waveform at traditional weighted average current



(b) Grid-connect current waveform with improved weighted average current

**Fig. 10** Grid-connect current waveform at  $L_g = 0$  mH. **a** Grid-connect current waveform at traditional weighted average current. **b** Grid-connect current waveform with improved weighted average current



In Fig. 7, it can be concluded that the closed-loop transfer function from  $i_{12\_d}$  to  $i_{ref\_d}$  is

$$G_{close} = \frac{i_{2\_d}}{i_{ref\_d}} = \frac{G_{ikPWM}}{L1(Lg + L2)Cs^2 + (L1 + Lg + L2)s + kckPWMS^2C(Lg + L2) + G_{ikPWM} - G_{fjPWMLgs}} \quad (17)$$

Equation (17) shows that the order of the system is relatively high and it is difficult to analyze the stabilization of the grid-connect current. Therefore, the control characteristics from  $i_{2\_d}$  to can be transformed into the control characteristics from  $i_{2\_d}$  to  $i_{ref\_d}$ , that is

$$\frac{i_{2\_d}}{i_{ref\_d}} = \frac{i_{2\_d}}{i_{12\_d}} \cdot \frac{i_{12\_d}}{i_{ref\_d}} \quad (18)$$

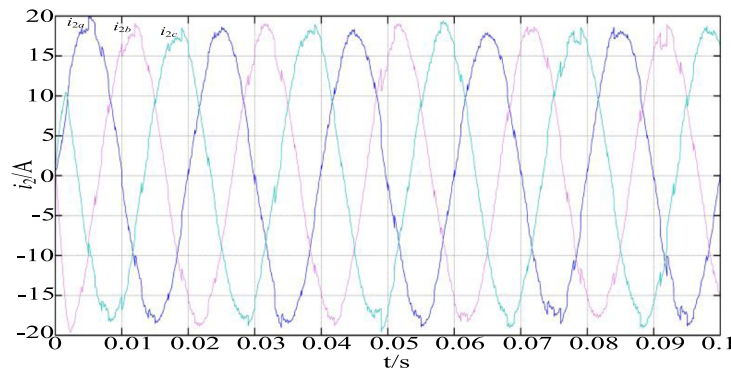
From eq. (16), we know that the open-loop transfer function from  $i_{12\_d}$  to  $i_{ref\_d}$  is a first-order form, and it is not affected by the impedance of the grid. Thus, the current control characteristics from  $i_{2\_d}$

to  $i_{ref\_d}$  are consistent with the those from  $i_{2\_d}$  to  $i_{12\_d}$ . In Fig. 7, the closed-loop transfer function of  $i_{2\_d}$  to  $i_{12\_d}$  can be

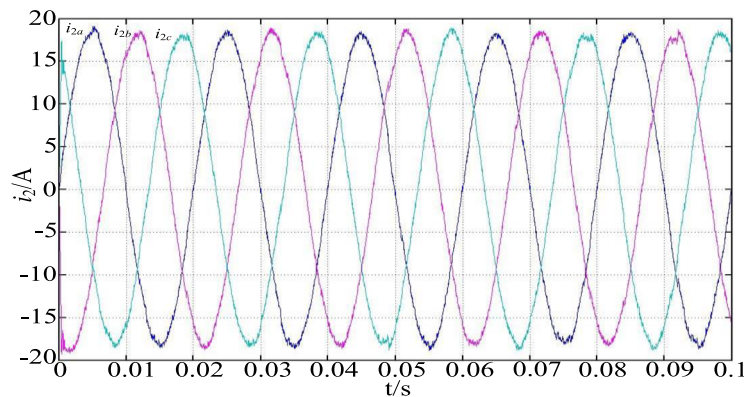
$$G_{close-g}(s) = \frac{i_{2\_d}}{i_{12\_d}} = \frac{1}{(1 - \alpha)(L_2 + L_g)Cs^2 + 2} \quad (19)$$

The Routh table of its closed-circus transfer function can be obtained from eq. (19), as shown in Tab. 2. It can be seen from the table that the first column is all positive, so the system is stable, and the current control characteristics from  $i_{2\_d}$  to  $i_{ref\_d}$  are consistent with the current control characteristics from  $i_{2\_d}$  to  $i_{12\_d}$ , so when the grid impedance occurs, only a small change of phase angle margin and amplitude margin of  $i_{2\_d}$  to  $i_{ref\_d}$  current control is made. But it is still within the allowable stability margin and the system operates stably.

In Fig. 7, the open-circus transfer function from  $i_{2\_d}$  to  $i_{ref\_d}$  is as follows



(a) Grid-connected current waveform when traditional weighted average current



(b) Improved weighted average current grid-connected current waveform

**Fig. 11** Grid-connected current waveform at  $L_g = 0.6$  mH. **a** Grid-connected current waveform when traditional weighted average current. **b** Improved weighted average current grid-connected current waveform

$$G_{close} = \frac{i_{2\_d}}{i_{ref\_d}} = \frac{G_{ikPWM}}{L1(L_g + L2)Cs^2 + (L1 + L_g + L2)s + kckPWMS^2C(L_g + L2) - G_{fkPWMLg_s}} \tag{20}$$

Through the eq. (20), the grid-connected current open-loop function Bode diagram with different grid impedances can be obtained in MATLAB, as shown in Fig. 9. The diagram tell us that when the grid impedance changes, the amplitude margin and phase margin from  $i_{2\_d}$  to  $i_{ref\_d}$  will change in a small range, but the system is still in stable operation.

**Simulation analysis**

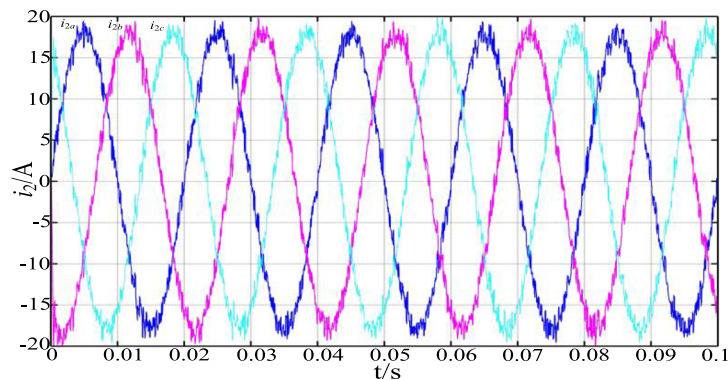
To prove the correctness of the control method, we propose, building grid connected inverter model in MATLAB. By selecting different grid impedance values for comparison, the simulation parameters are shown in Table 1, and the weighting coefficient is set to be  $\alpha = L2 / (L1 + L2) = 0.545$ .

Taking A-phase current as the analysis object, when the grid impedance  $L_g = 0$ , the grid is in a strong state. The grid current simulation diagram of the two

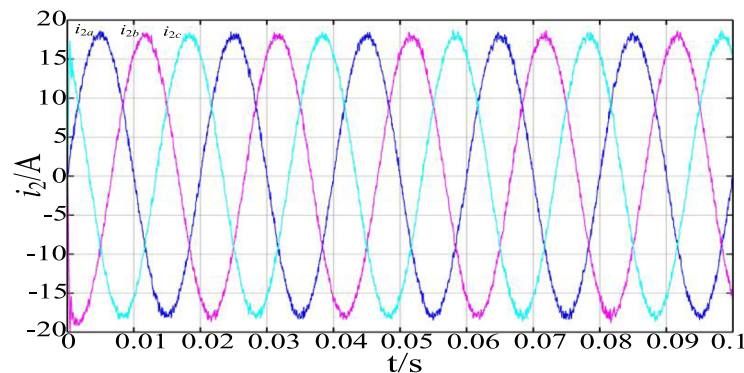
methods is shown in Fig. 10a and b, respectively. It can be find out from the figure that when the effect of grid impedance is ignored, both methods can operate stably with little difference, the waveform is smooth and convergent, and the output current quality of inverter is good.

When considering the grid impedance, 0.6 mH grid inductive reactance is connected in series at PCC, as shown in Fig. 11a and b. The waveform is obviously distorted after using the traditional weighted average current, the waveform is not smoothly convergent, and the THD is 4.6%. However, with the improved method, the waveform has no obvious distortion, only a few defects, and the waveform is basically smoothly convergent. The system can run stably, and THD is 2.2%. The output current quality of inverter is better.

When a 2 mH grid impedance is connected in series with PCC, the current weighted average traditional distortion becomes more serious. As shown in Fig. 12a, there are many waveform defects, the system is no longer stable, and the inverter output current quality is poor, at this time THD = 5.1%. After the improved method is adopted, the waveform has a little distortion



(a) Grid-connected current waveform at traditional weighted average current



(b) Grid-connected current waveform with improved weighted average current

**Fig. 12** Grid-connected current waveform at  $L_g = 2$  mH. **a** Grid-connected current waveform at traditional weighted average current. **b** Grid-connected current waveform with improved weighted average current

and few defects. Generally, it is smooth convergence, and the system can still operate stably with THD = 2.8%. The output current quality of the inverter is good.

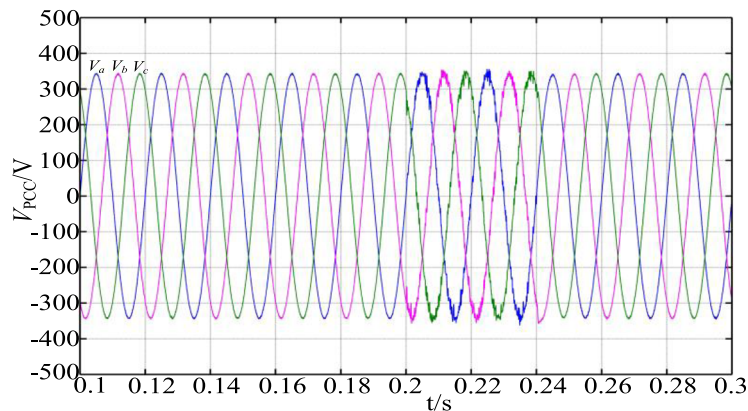
Figure 13 shows the emulation oscillogram of the switching process of traditional weighted average current and improved weighted average current when  $L_g = 2$  mH. The figure includes the voltage waveform of the common parallel node and the grid current waveform. Before 0.2 s, the grid-connect inverter adopts the improved weighted average current method. The output current waveform of the inverter is of good quality, contains less harmonics, and basically runs smoothly at 0.2 s. When switching to the traditional weighted average current method, it can be found that the grid-connect current waveform and voltage waveform have the phenomenon of oscillation and divergence, and the harmonic content is more, the system becomes unstable. At the time of 0.24 s, the improved weighted average current method is put into use again, the system slowly recovers from

an unstable state to a stable state, the waveform is smooth and converges, and the harmonic content is reduced.

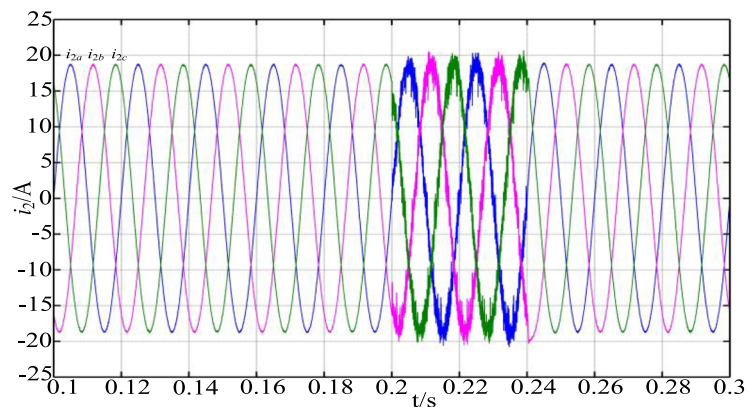
### Conclusion

The active damping control method based on grid voltage feed-forward is analyzed under the power network impedance. With the feed-forward control introduced, a regenerative feed-back circuit with grid impedance has been added from the merging node, which will reduce the stability of grid current control.

For reduce the influence of power network impedance, the weighted average current control method is added to the control method. The current control method deduces that the traditional weighting coefficient is related to the grid impedance. It needs to measure the change of the grid impedance at any time to correct the weighting coefficient, which makes the control system very complex.



(a) PCC voltage waveform of public grid connection point



(b) Grid-connected current waveform

**Fig. 13** Simulation waveform diagram of traditional and improved method switching process. **a** PCC voltage waveform of public grid connection point. **b** Grid-connected current waveform

In order to solve the shortcomings of the traditional weighting coefficient, an improved weighted average current method is proposed. By redesigning the weighting coefficient, the influence of the grid impedance is suppressed. System decreased from third-order to first-order, the stability of the grid impedance will not decrease, and the parameter calculation of the filter will directly obtain the weighting coefficient.

#### Acknowledgments

We would like to thank the anonymous reviewers for their valuable comments and suggestions, which helped improve the quality of this paper. Also, we want to express our heartfelt gratitude to the authors of the literature cited in this paper for contributing useful ideas to this study.

#### Authors' contributions

Li Shengqing determined the direction, designed experiments, collected literature, and wrote the first draft of the paper. Li Xinluo performed modeling, compared experimental results and collected data. Li Xiaobao rigorously reviewed the methods used to help structure and write the paper. The author(s) read and approved the final manuscript.

#### Funding

This work was supported in part by the National Natural Science Foundation of China under Grant 51977072, in part by the National Research and Development Program under Grant 2018YFB0606005, and in part by the Hunan Natural Science Foundation under Grant 2017JJ4024.

#### Availability of data and materials

All data generated or analyzed during this study are included in this article.

#### Competing interests

The authors declare that they have no competing interests regarding the publication of this manuscript.

Received: 23 September 2020 Accepted: 2 February 2021

Published online: 12 February 2021

#### References

- Fang T, Huang C, Chen N (2018) A phase-lead compensation strategy on enhancing robustness of LCL-type grid-tied inverters under weak grid conditions. *Trans China Electro-Technical Society* 33(20):4813–4822. <https://doi.org/10.19595/j.cnki.1000-6753.tces.171323>
- Liserre M, Teodorescu R, Blaabjerg F (2006) Stability of photovoltaic and wind turbine grid-connected inverters for a large set of grid impedance values. *IEEE Trans Power Electron* 21(1):263–272. <https://doi.org/10.1109/TPEL.2005.861185>
- Yang W, Chen Y, Zhou L (2018) Influence and stability analysis of small-interference modeling of three-phase LCL grid-connected inverter under weak grid. *Proceedings of the CSEE* 38(13): 3792–3804+4020. doi:<https://doi.org/10.13334/j.0258-8013.pcsee.171652>
- Wu H, Yan X, Yang D (2014) Study on the influence of phase-locked loop on the stability of LCL grid-connected inverter under weak grid conditions and the design of phase-locked loop parameter. *Chinese J Electrical Eng* 34(30):5259–5268. <https://doi.org/10.13334/j.0258-8013.pcsee.2014.30.001>
- Sun J (2011) Impedance-based stability criterion for grid-connected inverters. *IEEE Trans Power Electron* 26(11):3075–3078. <https://doi.org/10.1109/TPEL.2011.2136439>
- Mohamed Y (2011) Suppression of low-and high-frequency instabilities and grid-induced disturbances in distributed generation inverters. *IEEE Trans Power Electron* 16(12):3790–3803. <https://doi.org/10.1109/TPEL.2011.2161489>
- Shen G, Zhu X, Zhang J (2010) A new feedback method for PR current control of LCL-filter based grid-connected inverter. *IEEE Trans Ind Electron* 57(6):2033–2041. <https://doi.org/10.1109/TIE.2010.2040552>
- Shen G, Zhang J, Li X (2010) Current control optimization for grid-tied inverters with grid impedance estimation. 2010 Twenty-fifth annual IEEE applied power electronics conference and exposition. CA, USA
- Han Y, Li Z, Yang P (2017) Analysis and design of improved weighted average current control strategy for LCL-type grid-connected inverters. *IEEE*

- Transactions on Energy Conversion* 32(3):941–952. <https://doi.org/10.1109/TEC.2017.2669031>
- Li Y, Dai X (2010) Analysis of the influence of weak power grid on current hysteresis control of photovoltaic grid-connected inverter. *Low Voltage Apparatus* 20:8–13. <https://doi.org/10.3969/j.issn.1001-5531.2010.20.003>
- Zhou L, Zhang M, Ju X, He G (2013) Analysis of the influence of grid impedance on the stability of large-scale grid-connected photovoltaic system. *Proceedings of the CSEE* 34:34–41 CNKI:SUN:ZGDC.0.2013-34-007
- Xu J, Xie S, Tang T (2014) Adaptive current control of LCL filtered grid-connected inverter under weak power grid. *Proceed CSEE* 34(24):4031–4039. <https://doi.org/10.13334/j.0258-8013.pcsee.2014.24.006>
- Yang D, Ruan X, Wu H (2014) A virtual impedance method to improve the adaptability of LCL grid-connected inverters to weak grids, *Proceed Chinese Soc Electrical Eng.* 34(15):2327–2335. <https://doi.org/10.13334/j.0258-8013.pcsee.2014.15.00>
- Xu F, Tang Y, Gu W (2016) Research on resonant feedforward control strategy of LCL grid-connected inverter under weak grid conditions. *Proceed CSEE* 36(18):4970–4979+5122. <https://doi.org/10.13334/j.0258-8013.pcsee.150608>
- Zhao Q, Guo X, Wu W (2007) Research on control strategy for single-phase grid-connected inverter. *Proceed CSEE* 27(16):60–64
- Xu J, Xie S, Ting T (2014) Improved control strategy with grid-voltage feedforward for LCL-filter-based inverter connected to weak grid. *IET Power Electron* 7(10):2660–2671. <https://doi.org/10.1049/iet-pel.2013.0666>
- Bao C, Ruan X, Wang X (2012) Design of injected grid current regulator and capacitor-current-feedback active damping for LCL-type grid-connected inverter [C]// *proceedings of IEEE energy conversion congress and exposition, Raleigh*. In: North Car Wang CB et al (eds) *New method of parameter optimization for LCL filter of three-p. olina: IEEE*, pp 579–586
- Peña-Alzola R, Liserre M, Blaabjerg F (2014) A self-commissioning notch filter for active damping in a three-phase LCL-filter-based grid-tie converter. *IEEE Trans Power Electron* 29(12):6754–6761. <https://doi.org/10.1109/TPEL.2014.2304468>
- Wang B, Li S, Qu L (2018) Improvement and robustness analysis of the weighted average current control based on LCL grid-connected inverter. *Electrical Measurement Instrumentation* 55(4):78–86. <https://doi.org/10.3969/j.issn.1001-1390.2018.04.014>
- Timbus A, Liserre M, Teodorescu R (2009) Evaluation of current controllers for distributed power generation systems. *IEEE Trans Power Electron* 4(3): 654–664. <https://doi.org/10.1109/TPEL.2009.2012527>

#### Publisher's Note

Springer Nature remains neutral with regard to jurisdictional claims in published maps and institutional affiliations.

Submit your manuscript to a SpringerOpen® journal and benefit from:

- Convenient online submission
- Rigorous peer review
- Open access: articles freely available online
- High visibility within the field
- Retaining the copyright to your article

Submit your next manuscript at ► [springeropen.com](https://www.springeropen.com)